$/N-39$

$/655$

$\rho \partial \partial$

MODAL IDENTIFICATION OF A DEPLOYABLE SPACE TRUSS

Axel Schenk and Richard S. Pappa

MODAL IDENTIFICATION OF A DEPLOYABLE SPACE TRUSS

Axel Schenk*
Institute of Aeroelasticity
DLR, German Aerospace Research Establishment
Göttingen, West Germany

Richard S. Pappa
Spacecraft Dynamics Branch
NASA Langley Research Center
Hampton, VA, U.S.A.

Abstract: This paper summarizes work performed under a collaborative research effort between the National Aeronautics and Space Administration (NASA) and the German Aerospace Research Establishment (DLR, Deutsche Forschungsanstalt für Luft- und Raumfahrt). The objective is to develop and demonstrate advanced technology for system identification of future large space structures. Recent experiences using the Eigensystem Realization Algorithm (ERA) for modal identification of Mini-Mast are reported. Mini-Mast is a 20-meter-long deployable space truss used for structural dynamics and active-vibration-control research at the NASA Langley Research Center. Due to nonlinearities and numerous local modes, modal identification of Mini-Mast proved to be surprisingly difficult. Methods available with ERA for obtaining detailed, high-confidence results are illustrated.

1. INTRODUCTION

The difficulty of performing modal-identification tests depends significantly on the dynamic complexity of the structure. While identification of small, individual components is often simple and straightforward, identification of large, assembled structures can be much more difficult. Mode shapes can be highly coupled and nonintuitive, analytical predictions may be significantly inaccurate, and different excitation and identification methods will generate different results. As an example, a recent state-of-the-art modal test of the Upper Atmosphere Research Satellite (UARS) used 240 accelerometers to measure important degrees-of-freedom, required three weeks for data acquisition, and generated 197 different mode estimates (not all unique) using several different excitation and identification techniques (ref. 1). A comparison of experimental and pre-test analytical mode shapes showed significant differences based on cross-orthogonality calculations (ref. 2).

Future large space structures, such as Space Station Freedom, will be even more difficult than UARS to characterize experimentally (ref. 3). Overall size and the number of individual components will increase, clusters of modes with low frequencies will occur due to numerous flexible appendages, and ground tests will be affected to a greater degree by gravity and test-article suspension forces (ref. 4). Verification of analytical predictions will

---

* Visiting researcher at the Langley Research Center

require increased testing of large ccmponents, subassemblies, or scale models (ref. 5). Some form of on-orbit identification is also likely to be used (ref. 6). Recognizing the importance and difficulty of these new challenges, considerable research has been underway within NASA and DLR in the areas of improved ground test methods and system identification techniques for these future structures (refs. 7-10).

This paper begins with a brief overview of Mini-Mast, a laboratory deployable space truss, followed by a summary of data acquisition procedures and finite-element analytical predictions. The body of the paper discusses modal identification results obtained for Mini-Mast using the Eigensystem Realization Algorithm (ERA) (ref. 11). Examples are given of techniques available with ERA to develop high confidence in the identification results. These techniques are typically applied in sequence, with initial findings providing information to guide subsequent analyses. The paper closes with a summary of best identification results obtained for the primary modes of Mini-Mast.

2. MINI-MAST

Mini-Mast is a 20-meter-long, deployable/retractable truss located in the Structural Dynamics Research Laboratory at the NASA Langley Research Center. It is used as a ground test article for research in the areas of structural analysis, system identification, and control of large space structures. Constructed using graphite-epoxy tubes, titanium joints, and precision fabrication techniques, Mini-Mast was designed and built to the high standards typical of spaceflight hardware (ref. 12). The name "Mini-Mast" is derived from the name "MAST" given to a longer, 60-meter version of the same design once considered for a Space Shuttle-attached flight experiment.

The structure is deployed vertically inside a high-bay tower, cantilevered from its base on a rigid foundation. The total height is 20.16 meters, containing 18 bays in a single-laced pattern with every other bay repeating. The design uses a triangular cross section with vertices located on a circle of diameter 1.4 meters. During deployment, Figure 1, center-span hinges on the diagonal members latch to provide structural stability. This design, using mid-diagonal hinges, permits high packaging efficiency by allowing the diagonal members to fold into the center of the stack during storage. From a structural dynamics point of view, however, these massive hinges introduce many additional low-frequency modes. In particular, a total of 108 additional modes appear in the frequency range from approximately 15 to 20 Hz due to the x and y first-bending modes of each of the 54 diagonal members of the truss.

For Controls-Structures Interaction (CSI) experiments (ref. 13), two instrumentation platforms have been added to Mini-Mast at bays 10 and 18 (the tip). Three large torque-wheel actuators on the tip platform are used to provide active damping forces in these experiments. The combined mass of the actuators, 110.5 Kg, exceeds the total truss mass of 104.3 Kg. To offload this large tip weight, a 5-meter-long tensioned steel cable extends upward from the center of the tip platform.

3. DATA ACQUISITION

Figure 2 provides a summary of the data acquisition process. Multiple-input random

2

excitation and frequency response functions (FRFs) were used in this project (ref. 14). Multiple-input random excitation minimizes the influence of nonlinearities compared to other excitation methods (ref. 15). Uncorrelated, continuous random signals were applied for a period of 15 minutes simultaneously to each of three shakers. Displacement responses were measured together with the applied excitation forces. These time histories were processed into FRFs with 2560 spectral lines from 0 to 80 Hz. Fifty ensemble averages were made, applying standard Hanning window and overlap processing techniques. Inverse fast Fourier transformation (FFT^{-1}) was used to obtain impulse response functions (IRFs) for input to ERA. Digital filtering was used in some cases to allow ERA analyses in selected frequency bands of interest.

Figure 3 illustrates the orientation of the 3 shakers and 51 noncontacting displacement sensors used in the tests. The shakers are located circumferentially around the truss at bay 9, attached with flexible stingers to the "corner-body" joint at each vertex. The sensors are similarly located at the vertices of the truss, from bay 2 through bay 18, with the measurement axes aligned perpendicular to the corresponding face. A total of 102 response measurements in the global x and y directions were derived using a transformation of FRFs for the 51 skewed sensors, assuming that the triangular cross sections of the truss translate and rotate as rigid bodies. The sensors are eddy-current proximity devices having a resolution of approximately 2.5 micrometers. Displacement measuring devices were used rather than traditional accelerometers because they are capable of sensing both static and dynamic information. Static deflections were measured in a series of preliminary tests.

The three shakers at bay 9 are used as disturbance sources in the CSI experiments. Their locations were selected primarily to excite the low-frequency modes below 10 Hz. Although other shaker locations could excite higher-frequency modes better, no others were used in this work. Relocation of shakers would have interfered unacceptably with on-going CSI experiments.

4. NASTRAN ANALYTICAL PREDICTIONS

Using a NASTRAN finite-element model, a total of 153 modes are predicted to occur below 100 Hz, including 108 "local" modes between approximately 15 and 20 Hz due to bending of the 54 diagonal truss members. Figure 4 shows representative analytical mode shapes. For correlation with the experimental results, two plots of each shape were generated. The left-hand plots show the full, spatially complete mode shapes. These results contain information at the full 618 analytical grid points. The right-hand plots show a subset of these shapes considering only the 51 experimental grid points. The displayed amplitude of motion has been normalized in each plot based on the largest displacement among included degrees-of-freedom. Obviously, significant differences occur in the appearance of many of the modes when only the 51 measurement locations are considered. For instance, although Mode 7 primarily involves the bending of diagonal truss members, it appears as a global 3rd-bending mode when observed only at the sensor locations. Although undesirable, such ambiguities are not uncommon in modal tests of complex structures. It is often impossible, or impractical, to fully measure all structural components such as the individual truss members of Mini-Mast.

The degree of similarity of analytical mode shapes, as observed at the 51 measurement

locations (102 DOFs), was quantified using the Modal Assurance Criterion (MAC) (ref. 16). These results are plotted in Figure 5. Each row and column in the figure represents one NASTRAN mode, with the value of MAC indicated by the size of the darkened area at the intersection of the corresponding row and column. High correlation is thus expressed by large black blocks. Ideally, all of the off-diagonal terms of this matrix should be small to permit unambiguous pairing of experimental and analytical results.

Although Mini-Mast is fundamentally a simple cantilevered beam, the additional modes introduced by the instrumentation platforms, tip cable, and individual truss members cause the overall dynamic characteristics to be surprisingly complex. Furthermore, the dynamic properties are relatively nonlinear (not included in the NASTRAN model) due to friction and backlash in the numerous joints.

5. INITIAL ERA ANALYSIS

Typically at the beginning of each modal survey test, information concerning the entire frequency range of interest is sought. These initial analyses are always a compromise between accuracy and speed, particularly with large data sets that arise in testing complex structures. With ERA, the most straightforward way of processing large data sets is to include all data simultaneously in a single multiple-input, multiple-output analysis. The advantages of this approach are that a global, least-squares estimate is obtained using all available data and that data handling is minimized. Disadvantages include the fact that better identification results are possible for specific characteristics using alternative processing techniques and that computer time requirements for a single large job are usually greater than for a series of smaller jobs.

Results from an initial ERA analysis of Mini-Mast data, using all 306 IRFs simultaneously in a single analysis, are summarized in Table 1. Identified damped natural frequencies and damping factors, as well as several types of "accuracy indicators," are shown. Accuracy indicators are used in ERA to assess the quality of the identified modal parameters.

Two primary accuracy indicators available with ERA are the Extended Modal Amplitude Coherence (EMAC) and the Weighted Modal Phase Collinearity (MPC-W). EMAC measures the consistency of mode-shape components identified using data from the beginning of the analysis window with corresponding components identified using data extended past the primary analysis window. For each mode, an EMAC value is computed for every measurement. As a summary of the results, an average EMAC is then calculated for each mode. MPC-W measures the extent of phase angle deviations from the ideal monophase behavior of classical normal modes. A value of 100 percent indicates exact monophase behavior. With MPC-W, the magnitude of each mode-shape component is used to weight the corresponding phase result. This approach deemphasizes mode-shape components with small magnitudes, which typically possess a disproportionate amount of phase-angle scatter due to noise.

To provide a simpler method for distinguishing those modes identified with high confidence by both EMAC and MPC-W, these two indicators were recently combined into a single new parameter, referred to as the Consistent Mode Indicator (CMI). It is computed as simply the product of EMAC and MPC-W, and ranges from zero to 100 percent. High

4

CMI values indicate consistency of the identification results with the characteristics of classical normal modes, in terms of both eigenvalues and eigenvectors. CMI was introduced in the present investigation under the collaboration between NASA and DLR.

Modes identified with high confidence based on CMI are highlighted in Table 1. In this initial analysis, only 4 of the 45 identified modes have CMI values of at least 80 percent. Also, CMI results for the 15 global modes are widely distributed, ranging from a maximum of 97.44 percent for mode 1B-Y (1st bending in the y direction) to a minimum of only 0.09 percent for mode 4B-X (4th bending in the x direction). In Section 7, examples will be given of techniques available with ERA for improving such initial identification results. Doing so, CMI values for the global modes of Mini-Mast will be increased from an average of 65 percent in this initial analysis to an average of 86 percent, with 11 modes attaining a CMI of at least 80 percent.

The last parameter listed in Table 1 is the Modal Strength Ratio (MSR). MSR is computed by dividing the root-mean-square (rms) amplitude of each identified mode by the total rms value of the data included in the ERA data matrices. It provides a useful indication of the relative strength of each mode. With Mini-Mast, the five structural modes below 10 Hz have significantly larger displacement amplitude than the other modes, based on excitation applied with the shakers at bay 9. The appearance of an additional spurious mode at 0.862 Hz with high MSR but low CMI and negative damping is attributed to nonlinearities. A more detailed discussion of these nonlinear effects will be given in Section 7.3.

Correlation of experimental and predicted modal characteristics requires the comparison of mode shapes. Using the Modal Assurance Criterion (MAC), each of the 45 identified mode shapes from this initial ERA analysis was compared with each of the 153 NASTRAN modes below 100 Hz, considering only the 102 experimental degrees-of-freedom. The results are shown in Figure 6. As in Figure 5, the MAC value for each pair of modes is indicated by the size of the darkened area at the intersection of the corresponding row and column.

Several observations concerning these MAC results are highlighted in Figure 6. They are: (1) although there is a diagonal trend in the lower left corner, three experimental mode shapes correlate with only two first-bending modes of the NASTRAN model, (2) many NASTRAN modes correlate with several experimental modes in the local-mode cluster, similar to the results shown in Figure 5, (3) MAC values of upper-frequency bending and torsion modes are generally high, with the exception of Mode 5B-X, though not always unique, (4) experimental mode No. 34 at 60 Hz (attributed to electrical noise) disagrees with all NASTRAN-predicted mode shapes, and (5) some experimental modes at frequencies less than 80 Hz correlate with modes at frequencies higher than 80 Hz in the NASTRAN model.

6. OVERVIEW ERA ANALYSIS

All identification results discussed in Section 5 were obtained in an initial ERA analysis using 50 assumed modes. For research purposes, identification results were also calculated in this investigation using a wide range of up to 125 assumed modes, realized by increasing the number of retained singular values up to 250. These results are referred to as the overview analysis.

The natural frequencies identified as a function of the assumed number of modes are plotted in Figure 7. Each row in this figure corresponds to a separate ERA analysis. The confidence of each result is expressed by the length of the vertical dashes, drawn proportional to the corresponding CMI value for the mode, with 100 percent represented by the distance between tic marks on the y-axis. High confidence is thus placed on modes appearing as continuous vertical lines, and lower confidence on modes appearing as dotted or dashed lines.

With the exception of mode 4B-X, all global modes are well identified. At high numbers of assumed modes, however, some additional weak modes appear in the mid-frequency range between 24 and 65 Hz. Also, a second cluster of local modes appears at frequencies between 69 and 80 Hz, attributed to the bending of the longeron truss members. These high-frequency, local characteristics are not accurately predicted by the finite-element model used in this study which represents each longeron member using only a single element. Another difference with NASTRAN predictions is that mode 5T is much closer in frequency to mode 5B-Y in the experimental results. Finally, typical of experimental data, a 60-Hz mode with zero damping is identified, assumed to be electrical noise. In summary, approximately 55 assumed modes are necessary to identify the 15 global truss modes between 0 and 80 Hz. This relatively high number of assumed modes necessary for identification of all global modes is caused primarily by mode 4B-X being more weakly excited than numerous local modes.

To examine in more detail the experimental results from the overview analysis, expanded views of Figure 7 in selected frequency intervals are presented in Figures 8 and 9. In addition to the identified frequencies, corresponding results for damping and MPC-W are also shown.

Figure 8 provides results for the frequency interval from 4 to 7 Hz, including modes 1T, 2B-X and 2B-Y. Three different regions can be identified as a function of the assumed number of modes. After an initial region of convergence below 40 assumed modes, an area of relative stability occurs up to approximately 75 assumed modes. This region is followed by a second area of instability, particularly in the damping results for modes 1T and 2B-X. Also, several spurious modes with low confidence are identified. Identification of the three global modes in this frequency range is optimum using a singular value truncation value of approximately 60 assumed modes.

Another frequency interval, containing modes 5B-X, 5B-Y and 5T, is shown in Figure 9. Here, only two separate regions are observed as a function of the assumed number of modes. At lower numbers of assumed modes, considerable identification scatter occurs, particularly in the MPC-W results. All results stabilize, however, at approximately 90 assumed modes. Moreover, no spurious modes occur as in Figure 8, with stability maintained all the way up to 125. In general, the best identification results for these three global modes are obtained using the full 125 assumed modes.

In summary, these typical results illustrate the difficulty of selecting a single, optimum singular-value cutoff with complex experimental data. Accuracy varies considerably from mode to mode, with no single selection of singular-value cutoff being optimum for all modes.

7. IMPROVEMENT OF RESULTS

With simple structures, identification methods typically generate accurate results in a single analysis. With complex structures, however, significant differences can occur among different analyses. In such cases, tools for ensuring accuracy and reliability of the results are needed. ERA offers several techniques for improving estimates of structural modal parameters, examples of which are discussed in this section.

With Mini-Mast, considerable uncertainty was encountered in the initial and overview analyses with 5 of the 15 global modes, namely modes 1B-X, 1B-Y, 4B-X, 5B-X and 5T. For modes 1B-X and 1B-Y, three modes were consistently identified rather than only two. This difficulty is attributed to nonlinearities. Previous data, such as frequency response functions generated using sine excitation, indicated that these fundamental bending modes are appreciably nonlinear due to friction and backlash in the joints. With mode 4B-X, the identification results were weak and uncertain. The problem here is low response level, attributed to a node line occurring near the shakers. As mentioned earlier, only a single set of shaker positions was available due to on-going CSI experiments. Mode 5B-X was identified with good confidence (CMI of 50 percent in the initial analysis); however, the MAC value between identified and NASTRAN shapes was only 26 percent—considerably lower than for the other modes. In the overview analysis, the frequency of mode 5T was found to be identical to that of mode 5B-Y. Additional analyses are needed to substantiate this result.

Many techniques are available with ERA to improve identification results for complex structures. These include:

1. Digital filtering.

2. Selection of emphasized data.

3. Multiple-input versus single-input analysis.

4. Sliding time-window analysis.

The first technique, digital filtering, is a generic capability used in conjunction with the others. Examples of each of the last three techniques are presented individually in the remainder of the paper.

7.1. Selection of Emphasized Data

Figure 10a provides an expanded view of frequency, damping and MPC-W near mode 4B-X from the overview analysis, using data for all three shakers and including all 102 response measurements. Considerable scatter is evident in these results, particularly in the damping values. Furthermore, the minimum number of assumed modes at which each mode is identified is relatively high. In this result, mode 3T is first identified at 20 assumed modes, mode 4B-X at 53 assumed modes, and mode 4B-Y at 16 assumed modes.

Improvement can be achieved by emphasizing measurements with the largest vibration amplitudes in the modes of interest. This approach provides an increased signal-to-noise ratio for the target modes. Results obtained by emphasizing data from sensors at bays 5,

7

6, 12 and 16 are shown in Figure 10b. Improvement of all three modes is clearly indicated. Initial identification of all modes occurs at smaller numbers of assumed modes (3T at 10, 4B-X at 37, and 4B-Y at 7), and CMI values, indicated by the lengths of the dashes in the left-hand plots, are uniformly higher. Also, all damping factors are much more stable. Based on these results an improved damping estimate for mode 4B-X of 2.0 percent was obtained.

In summary, a significant improvement can be achieved by emphasizing measurements corresponding to larger vibration amplitudes. This procedure requires estimates of the mode shapes for the modes of interest. Mode-shape estimates were obtained in this example using the initial identification results.

7.2. Multiple-Input versus Single-Input Analysis

In theory, ERA will identify repeated or closely spaced eigenvalues of multiplicity m, having m independent eigenvectors, when data for at least m linearly independent inputs and outputs are included in the analysis. In practice, however, data inconsistencies can cause difficulties for multiple-input, multiple-output analyses. For example, when data acquired in different tests of the same structure are analyzed simultaneously, slight changes in eigenvalues or eigenvectors between data sets can cause additional modes to be identified. Such inconsistencies are not uncommon in laboratory tests due to nonlinearities or small variations of physical properties with time.

To assess the extent of such inconsistencies, ERA analyses were performed using various combinations of shakers[†].   Figure 11 shows typical results obtained in the frequency interval from 66 to 68 Hz. Using only a single shaker, Figure 11a, two modes are clearly identified. Although the frequency and damping results are stable, MPC-W values for the higher-frequency mode (labeled 5B-Y) are only about 70 percent. Also, when MAC values are computed between the identified and NASTRAN mode shapes (not shown), this mode correlates approximately 50 percent with NASTRAN mode 5B-Y *and* approximately 25 percent with NASTRAN mode 5T. The explanation for this behavior is that the identified mode labeled "5B-Y" is, in fact, a linear combination of the two actual modes. The two modes are so closely spaced in frequency that a single-input analysis is unable to separate them.

Figure 11b shows the improved results obtained using data for all three shakers simultaneously.   Two modes at essentially the same frequency (within 0.001 Hz) are now identified. All results, including the MPC-W values, stabilize at approximately 45 assumed modes. Also, MAC values computed with the NASTRAN shapes (not shown) now show unique correlation. In particular, the modes labeled 5B-Y and 5T each correlate approximately 60 percent with their corresponding NASTRAN predictions. Moreover, the cross-correlation of shapes between the two pairs is now approximately zero, indicating linear independence. These identification results shown in Figure 11b were obtained using three shakers and emphasized data. Similar results were obtained in the overview analysis, Figure 9, except that a much higher number of assumed modes was required.

---

† Clarification of this terminology is required. All data analyzed in this project were obtained in a single test conducted using all three shakers. An "ERA analysis performed using various shakers" refers to the process of analyzing simultaneously a subset of this data corresponding to various shakers. The expressions "single-shaker" and "multiple-shaker" are used synonymously with "single-input" and "multiple-input," respectively.

In summary, multiple-input analysis provides a clear advantage over single-input analysis for identification of modes 5B-Y and 5T.

7.3. Sliding Time-Window Analysis

Most identification techniques, including ERA, are based on the assumption of linear structural behavior. However, all mechanical structures are nonlinear to some degree. Nonlinearities can significantly affect modal identification results, particularly with closely spaced modes. Random excitation with averaging was used in the Mini-Mast tests to minimize these effects. Although this approach generates the best linear estimates of FRFs (ref. 15), residual nonlinear effects can remain.

A sliding time-window analysis was performed using ERA to characterize these residual effects. The method is illustrated in Figure 12 with a typical Mini-Mast IRF. Beginning at the data interval labeled "1," an initial ERA analysis was performed. Then, using a time shift of 6 data samples (0.3 sec.), the interval was moved down the IRF and a second ERA analysis performed. This process was repeated 50 times for a total time shift of 15 seconds. With linear data, the identified modal parameters remain constant among these separate analyses. Nonlinearities or other data distortions, however, cause changes to occur. The objective is to determine the nature and size of these changes.

Digital filtering was applied from 0 to 10 Hz to concentrate the analyses on the low-frequency global modes. Frequency, damping, and MPC-W results obtained for modes 1B-X and 1B-Y as a function of time shift are discussed in this section. Also shown are representative MAC values calculated between the identified mode shapes and each of the first five NASTRAN-predicted mode shapes.

Identification results obtained using data for all three shakers simultaneously are shown in Figure 13. As in the initial and overview analyses, three modes are consistently found. Based on CMI, indicated by the height of the dashes in the left-hand plot, the confidence of these results varies randomly, and the frequencies scatter throughout the entire 0.8 to 0.9 Hz interval. The damping as well as the MPC-W values also show large scatter, including negative damping estimates. Typical MAC values are plotted in the right-hand figure. NASTRAN mode 1 (1B-X) is clearly identified in this result while NASTRAN mode 2 (1B-Y) is identified twice, by experimental modes 1 and 3. Additionally, however, these MAC values vary considerably among the 50 separate analyses that were performed (not shown). At other time shifts, completely different mixtures of correlation with the two NASTRAN modes were obtained for the three identified modes. MAC results for Mode 1T and both 2nd-bending modes in the upper frequency range are high and correlate uniquely with NASTRAN predictions in all cases.

Next, results obtained using one of three possible combinations of two shakers are shown in Figure 14. Only two modes are identified and frequencies are relatively stable. However, a strong nonlinear characteristic is now clearly observed in the damping results. The identified damping factors increase uniformly from approximately 1 percent at zero time shift to approximately 4 percent at a time shift of 15 seconds. Overall, these frequency and damping results obtained using two shakers are significantly more stable and understandable than those shown in Figure 13 using three shakers. MPC-W results, however, continue to have considerable scatter. Also, MAC results show a consistent pattern of modal coupling

with the first two NASTRAN modes. MAC values again vary among the 50 separate analyses; however, the variation is smaller than with three shakers. In general, each of the two identified mode shapes obtained in this analysis is a linear combination of the first two NASTRAN mode shapes. This coupling of identified modes is attributed to the effects of nonlinearities, combined with the close spacing of natural frequencies. MAC results for modes 3 through 5 are again high and correlate uniquely with corresponding NASTRAN modes. Similar results are obtained using the two other combinations of two shakers.

For the final set of analyses, data for each shaker were used individually. Results obtained using data for shakers 2 and 3 are shown in Figures 15a and 15b, respectively. As with two shakers, the identified frequencies are fairly stable while damping factors again show an increasing nonlinear characteristic. Also, decreasing patterns are observed in the MPC-W results for both cases. These trends are normal and are attributed to the decreasing signal-to-noise ratio of each mode versus time. Most importantly, however, is that consistently high and unique MAC values for modes 1B-X and 1B-Y are now obtained. Furthermore, these MAC results vary only slightly among the 50 separate analyses. Using data for shaker 1 only (not shown), a coupled mode shape was typically identified, similar to those found using two shakers.

In summary, single-input data analysis provided improved results for the first two modes of Mini-Mast compared to multiple-input analysis due to nonlinearities. When data for all three shakers were used simultaneously, a spurious third mode was consistently identified. Using data for only two shakers generally eliminated the spurious mode, but identified mode shapes were highly coupled. The largest MAC values with NASTRAN predictions were consistently obtained using data for shakers 2 and 3 individually to identify modes 1B-Y and 1B-X, respectively.

8. SUMMARY OF IDENTIFICATION RESULTS

Final identification results for all global modes of Mini-Mast below 80 Hz are listed in Table 2, together with their best CMI values. For comparison with the NASTRAN model, the predicted frequencies and mode shape correlation based on MAC are also shown. Due to nonlinearities, frequency ranges for the first two modes and damping-factor ranges for the first five modes are given. Beyond 10 Hz, all modes are assumed to be linear.

Each of the 15 global modes, except mode 4B-X, was identified with good confidence based on CMI. Corresponding MAC values are also relatively high, although a trend of decreasing correlation with increasing frequency is clearly evident. In general, natural frequencies and damping factors were all well identified, including those for modes 5B-Y and 5T which have virtually identical frequencies. The only exception is the damping result for mode 4B-X, which has reduced confidence indicated by the low CMI value. Overall, the NASTRAN predictions agreed closely with the experimental results, the largest difference in frequency being 8.3 percent for mode 5T.

These final identification results were selected from among all analyses performed in this project. The selections correspond to the largest CMI values obtained in all analyses, unless the corresponding MAC value was unusually low.

10

9. CONCLUSIONS

The work discussed in this paper was conducted under a collaborative research agreement between NASA and DLR in the area of Dynamics and Control of Large Space Systems. The objective is to advance the state-of-the-art in system identification and validation of structural analytical models. Validated analytical models of future large spacecraft are essential to assuring on-orbit performance and for designing and operating control systems.

Based on the experiences encountered in this project, the following general conclusions are reached:

o With complex, future large space structures, the selection and placement of a minimum number of sensors can considerably affect the correlation of analytical and experimental modal parameters. In particular, multiple modes with similar shapes at the test degrees-of-freedom may occur if significant motions are unmeasured.

o The theoretical advantages of multiple-input data analysis with closely spaced modes are disrupted by nonlinearities or other data inconsistencies. Classical single-input analysis may offer better understanding in such situations.

o A variety of different methods can be used to improve the accuracy of particular identified parameters, perhaps at the expense of others. The methods illustrated in this paper generated considerable improvements with Mini-Mast data; however, they require further development to become routine capabilities.

o The Consistent-Mode Indicator (CMI) developed in this project reliably indicates modes with classical normal-mode behavior, both in theory and in practice. Values greater than 80 percent correspond to modes identified with high confidence.

10. REFERENCES

1 Eckles, W. and Garnek, M., "The Upper Atmosphere Research Satellite Modal Test," Proceedings of the 60th Shock and Vibration Symposium, Virginia Beach, VA, November 1989, Volume 2, pp. 45-60.

2 Eckles, W., Breskman, D. and McMullan, J., "UARS Mechanical Test Model Dynamic Test Final Report. Volume 1: Modal Test," GE Astro Space Report 1R44-UARS-PIR-1697, August 1989, Table 6.1.1.

3 Pappa, R. S., "Identification Challenges for Large Space Structures," *Sound and Vibration*, April 1990, pp. 16-21.

4 Hanks, B. R. and Pinson, L. D., "Large Space Structures Raise Testing Challenges," *Astronautics and Aeronautics*, October 1983, pp. 34-40.

5 McGowan, P. E., Edighoffer, H. H. and Wallace, J. W., "Development of an Experimental Space Station Model for Structural Dynamics Research," Proceedings of the 60th Shock and Vibration Symposium, Virginia Beach, VA, November 1989, Volume 2, pp. 13-29.

[6] Cooper, P. A. and Johnson, J. W., "Space Station Freedom On-Orbit Modal Identification Experiment—An Update," Presented at the 2nd USAF/NASA Workshop on System Identification and Health Monitoring of Precision Space Structures, Pasadena, CA, March 1990.

[7] Venneri, S. L., Hanks, B. R. and Pinson, L. D., "Future Trends in Spacecraft Design and Qualification," AGARD CP-397, *Mechanical Qualification of Large Flexible Spacecraft Structures*, September 1985.

[8] Wada, B. K., Kuo, C. P. and Glaser, R. J., "Multiple Boundary Condition Tests (MBCT) for Verification of Large Space Structures," AIAA Paper 86-0905, May 1986.

[9] Hornung, E., Breitbach, E. and Öry, H., "Recent Developments and Future Trends in Structural Dynamic Design Verification and Qualification of Large Flexible Spacecraft," AGARD CP-397, *Mechanical Qualification of Large Flexible Spacecraft Structures*, September 1985.

[10] Schenk, A., "Modal Analysis of Space Structures With the Ibrahim Time Domain Method," ESA SP-289, Proceedings of International Conference on Spacecraft and Mechanical Testing, Noordwijk, The Netherlands, October 1988.

[11] Juang, J.-N. and Pappa, R. S., "An Eigensystem Realization Algorithm for Modal Parameter Identification and Model Reduction," *Journal of Guidance, Control and Dynamics*, Vol. 8, No. 5, September-October 1985, pp. 620-627.

[12] Adams, L. R., "Design, Development and Fabrication of a Deployable/Retractable Truss Beam Model for Large Space Structures Applications," NASA CR-178287, Astro Aerospace Corporation, June 1987.

[13] Hanks, B. R., "Controls-Structures Interaction, An Interdisciplinary Challenge for Large Spacecraft," Proceedings of the 35th American Astronautical Society Symposium, St. Louis, MO, October 1988.

[14] Allemang, R. J., Rost, R. W. and Brown, D. L., "Multiple Input Estimation of Frequency Response Functions: Excitation Considerations," ASME Paper 83-DET-73, 1983.

[15] Olsen, N. L., "Excitation Functions for Structural Frequency Response Measurements," Proceedings of the 2nd International Modal Analysis Conference, Orlando, FL, February 1984, pp. 894-902.

[16] Allemang, R. J. and Brown, D. L., "A Correlation Coefficient for Modal Vector Analysis," Proceedings of the 1st International Modal Analysis Conference, Orlando, FL, November 1982, pp. 110-116.

NO.		HERTZ	FACTOR,%	CMI,%	EMAC,%	MPC-W	MSR,%
1B-X?	1	0.827	3.880	78.10	89.08	87.67	27.9
	2	0.862	-0.950	3.09	97.16	3.18	80.8
1B-Y	3	0.867**	1.243	97.44**	97.86	99.57	73.7
	4	3.319	54.501	0.00	0.01	32.65	0.6
1T	5	4.187**	1.424	96.87**	97.17	99.69	24.5
2B-X	6	6.118*	2.053	94.80*	96.12	98.63	31.1
2B-Y	7	6.175+	0.993	88.18+	94.45	93.36	35.0
	8	13.298	27.099	0.00	0.00	30.64	0.6
	9	14.062	1.961	37.70	43.20	87.27	1.4
	10	15.325	2.157	13.86	35.73	38.79	1.5
	11	15.897	1.225	42.90	65.45	65.54	4.7
	12	16.361	1.320	26.27	65.23	40.28	4.3
	13	16.460	5.508	12.75	17.51	72.82	5.2
	14	16.682	2.413	10.00	42.04	23.78	1.0
	15	17.381	1.957	57.99	63.86	90.82	5.3
	16	18.905	18.756	0.00	0.00	46.59	0.8
	17	19.607	1.793	19.92	26.04	76.50	1.5
	18	20.349	5.896	0.38	0.72	52.90	1.5
	19	20.636	0.916	8.06	38.56	20.90	0.8
	20	21.396	1.914	7.49	11.07	67.71	0.8
	21	21.518	3.683	0.42	17.00	2.45	0.9
	22	22.372	58.914	0.00	0.00	9.82	0.5
2T	23	22.891	0.949	76.60	81.94	93.48	7.4
3B-X	24	31.137	1.780	60.83	68.66	88.59	3.4
3B-Y	25	32.410	1.935	64.32	76.82	83.72	3.1
	26	35.671	20.831	0.00	0.00	4.78	0.4
3T	27	38.126	1.250	44.97	51.42	87.45	1.0
	28	40.172	4.872	0.09	0.18	49.61	0.5
4B-Y	29	43.315	0.701	56.57	67.72	83.54	1.7
	30	45.000	7.852	0.00	0.00	16.53	0.3
	31	51.059	9.683	0.00	0.00	33.70	0.5
4T	32	51.563	0.705	73.77	91.52	80.60	6.1
	33	55.748	1.029	12.54	16.34	76.74	0.4
	34	60.070	0.102	29.34	41.06	71.46	0.4
5B-X	35	66.886	0.382	50.39	60.33	83.53	1.9
5T	36	67.079	0.560	27.56	59.13	46.60	1.7
5B-Y	37	67.225	0.393	72.91	86.87	83.94	2.5
	38	69.017	2.458	0.27	0.50	52.85	0.9
	39	70.245	0.649	3.08	52.66	5.84	0.7
	40	70.792	0.324	12.20	64.77	18.84	1.4
	41	71.119	1.272	1.22	7.67	15.90	0.9
	42	71.233	0.794	15.33	26.07	58.79	0.8
	43	73.946	1.321	0.69	1.75	39.70	0.3
	44	76.647	2.304	0.02	0.19	12.55	0.3
	45	79.558	0.846	32.16	37.14	86.60	1.3

SUMMARY

CMI RANGE	KEY	NO. OF MODES
95% - 100%	**	2
90% - 95%	*	1
80% - 90%	+	1
0% - 80%		41

1B-X = 1st X bending
1B-Y = 1st Y bending
1T = 1st torsion
etc.

Table 1. Initial ERA Results

Mode		NASTRAN		TEST			
	Mode No.	Frequency [Hz]	Frequency [Hz]	Damping [%]	Best CMI [%]	MAC [%]
1st X-bending	1	0.798	0.856-0.870*	1.0-4.0*	87.4	94.1
1st Y-bending	2	0.800	0.862-0.868*	1.0-4.0*	97.4	98.9
1st torsion	3	4.37	4.19	1.3-1.9*	98.3	98.9
2nd X-bending	4	6.11	6.11	2.0-2.5*	96.8	92.1
2nd Y-bending	5	6.16	6.18	1.1-1.4*	97.1	97.1
2nd torsion	118	21.57	22.89	0.82	92.5	92.2
3rd X-bending	121	30.72	31.16	1.56	83.8	90.0
3rd Y-bending	122	32.06	32.39	1.36	73.1	76.8
3rd torsion	127	39.01	38.06	0.83	79.7	85.9
4th X-bending	128	42.22	40.42	1.99	55.7	89.8
4th Y-bending	129	44.86	43.23	0.43	82.2	74.4
4th torsion	130	54.27	51.55	0.74	79.4	65.8
5th X-bending	134	69.87	66.92	0.44	90.2	32.1
5th Y-bending	135	70.18	67.27	0.33	88.0	56.4
5th torsion	137	72.87	67.27	0.57	80.9	60.7

* due to nonlinearity
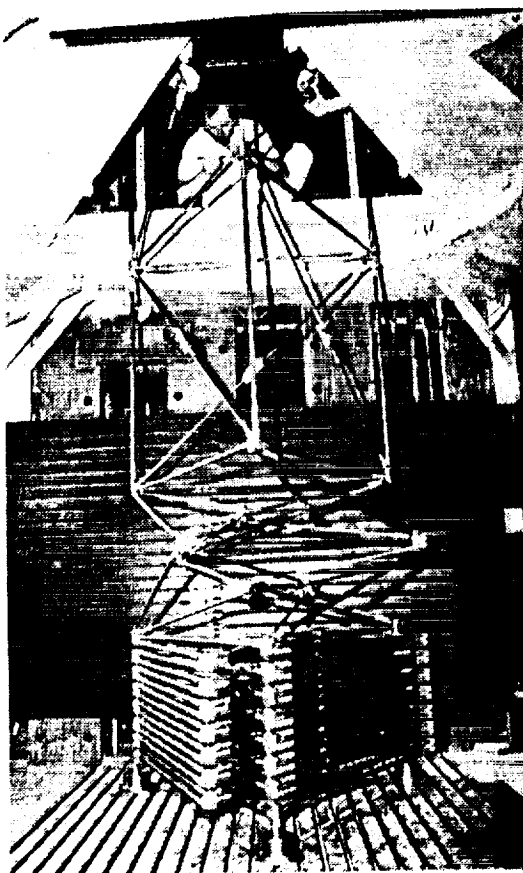
Table 2. Best Identification Results for Global Modes
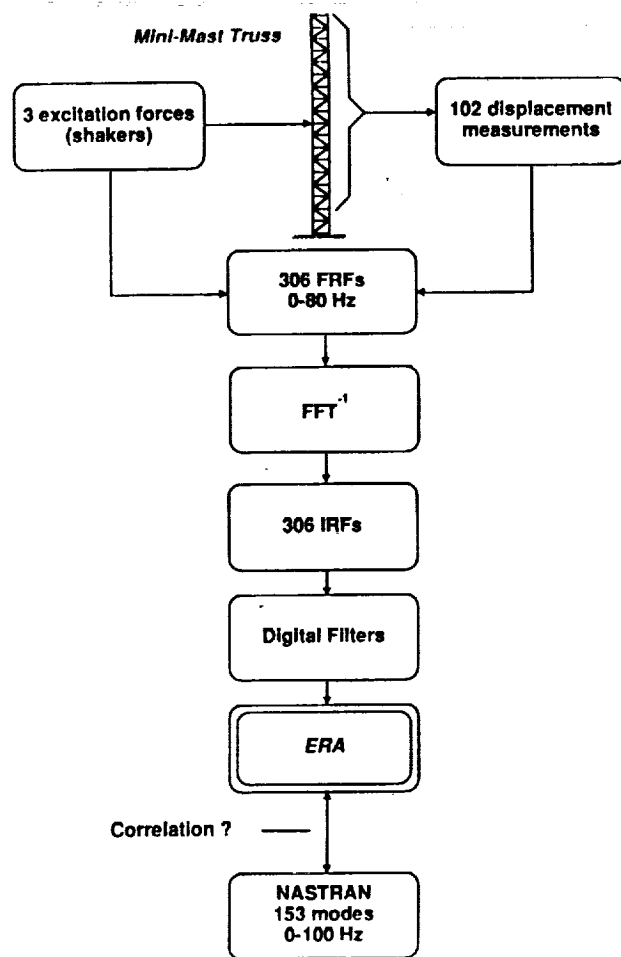
13

Figure 1. Mini-Mast, Deployment Process

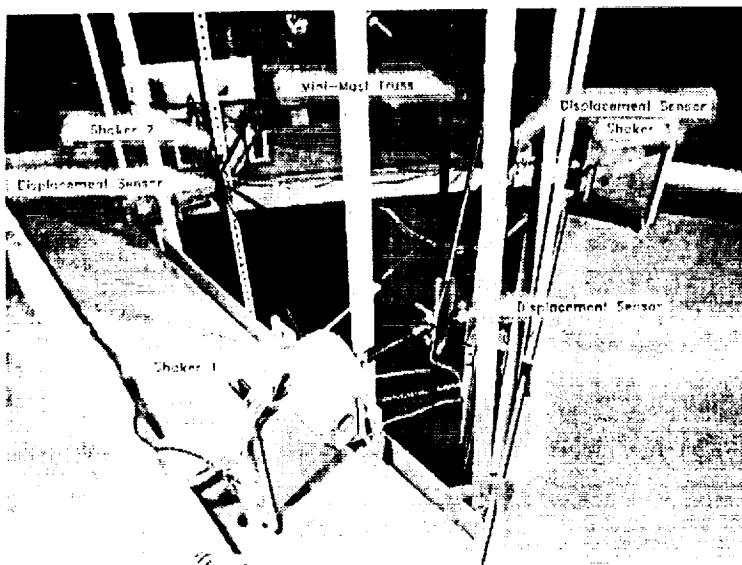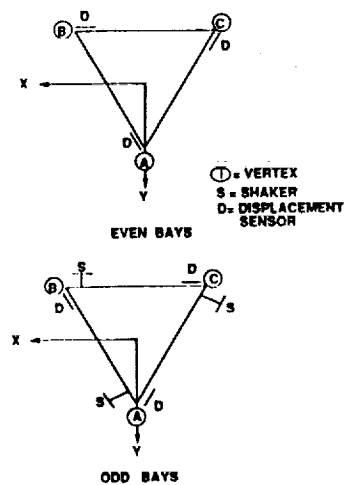Figure 2. Data Acquisition Overview
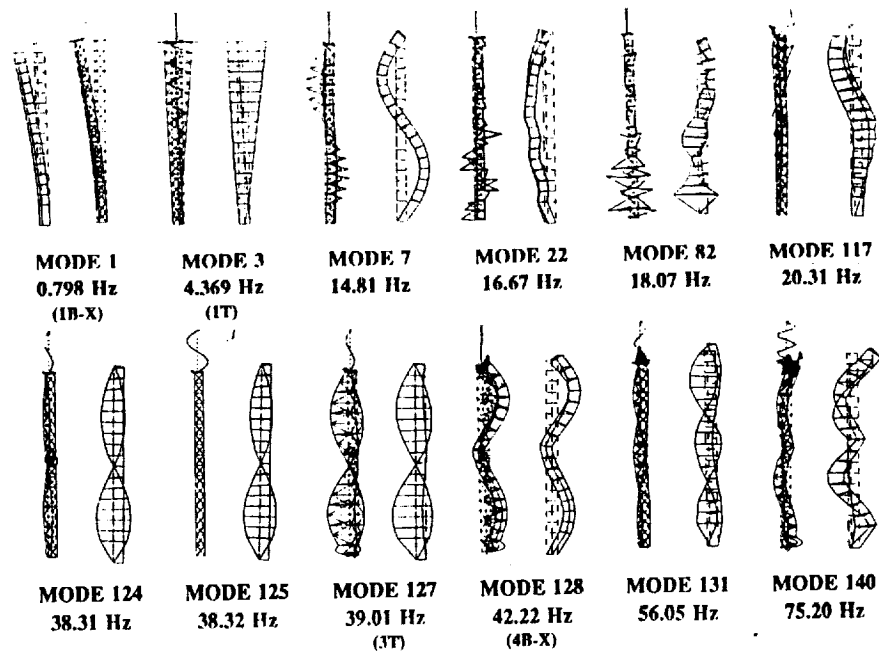
Figure 3. Orientation of Shakers and Sensors

14

Figure 4. Representative NASTRAN Mode Shapes
Left: Full Mode Shapes (618 Nodes), Right: At Sensor Locations Only (51 Nodes)
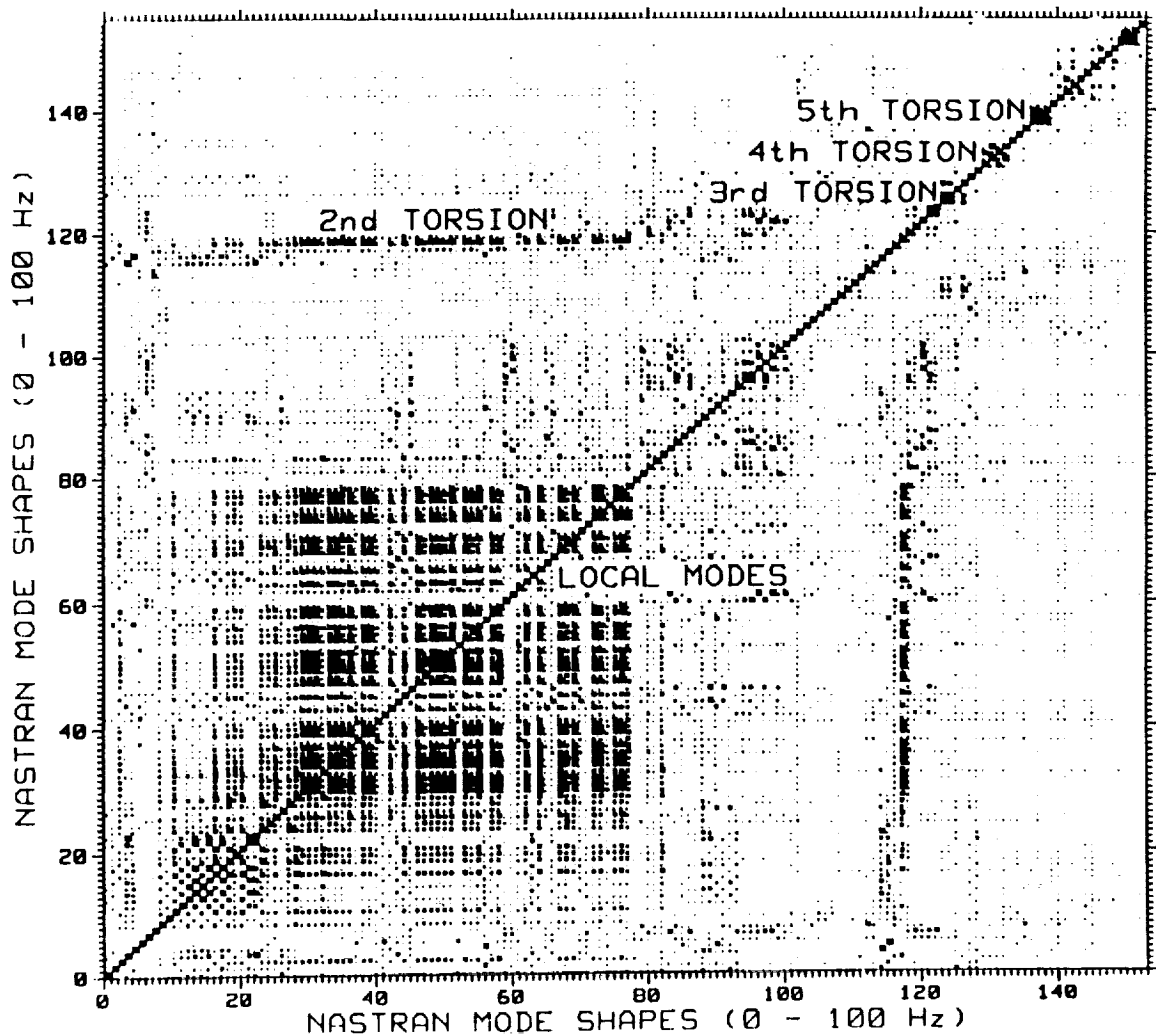

Figure 5. Self-Correlation of NASTRAN Mode Shapes
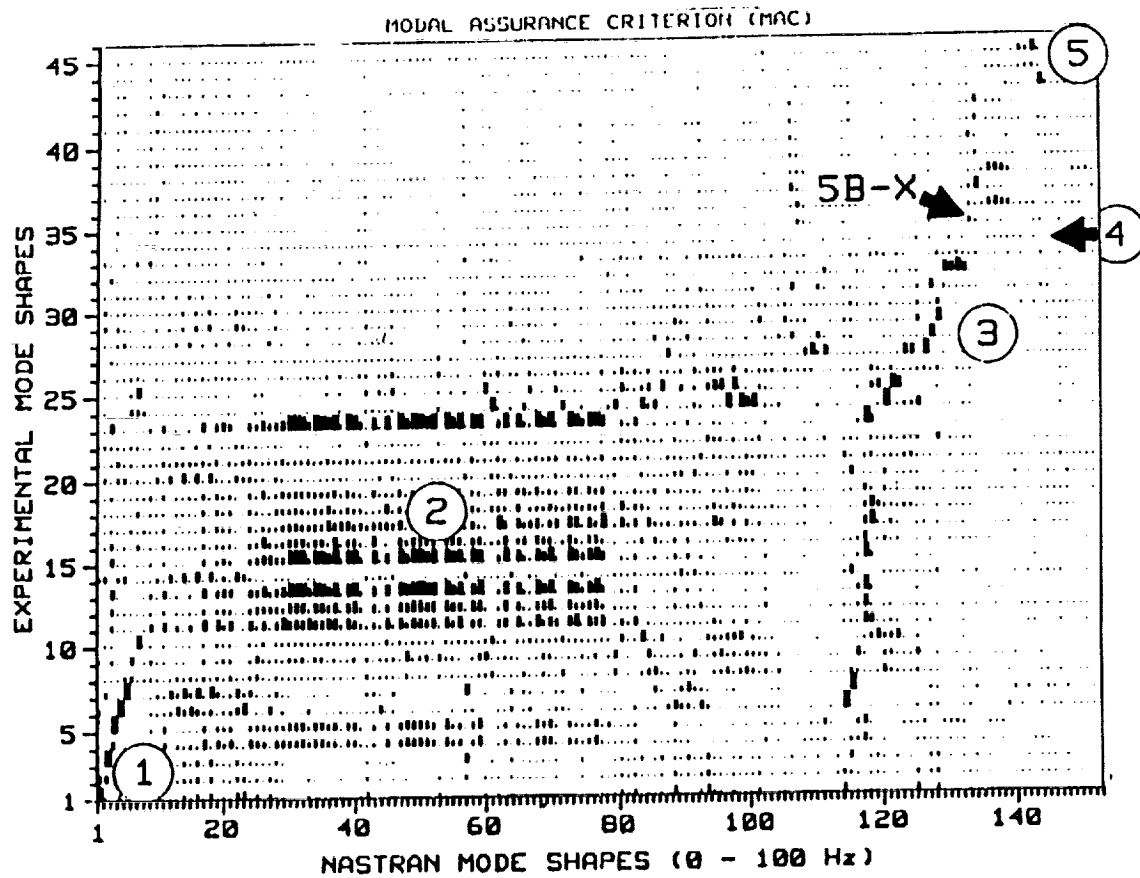at Test Degrees-of-Freedom (102 DOFs), Using MAC

15

Figure 6. Correlation of Identified Mode Shapes
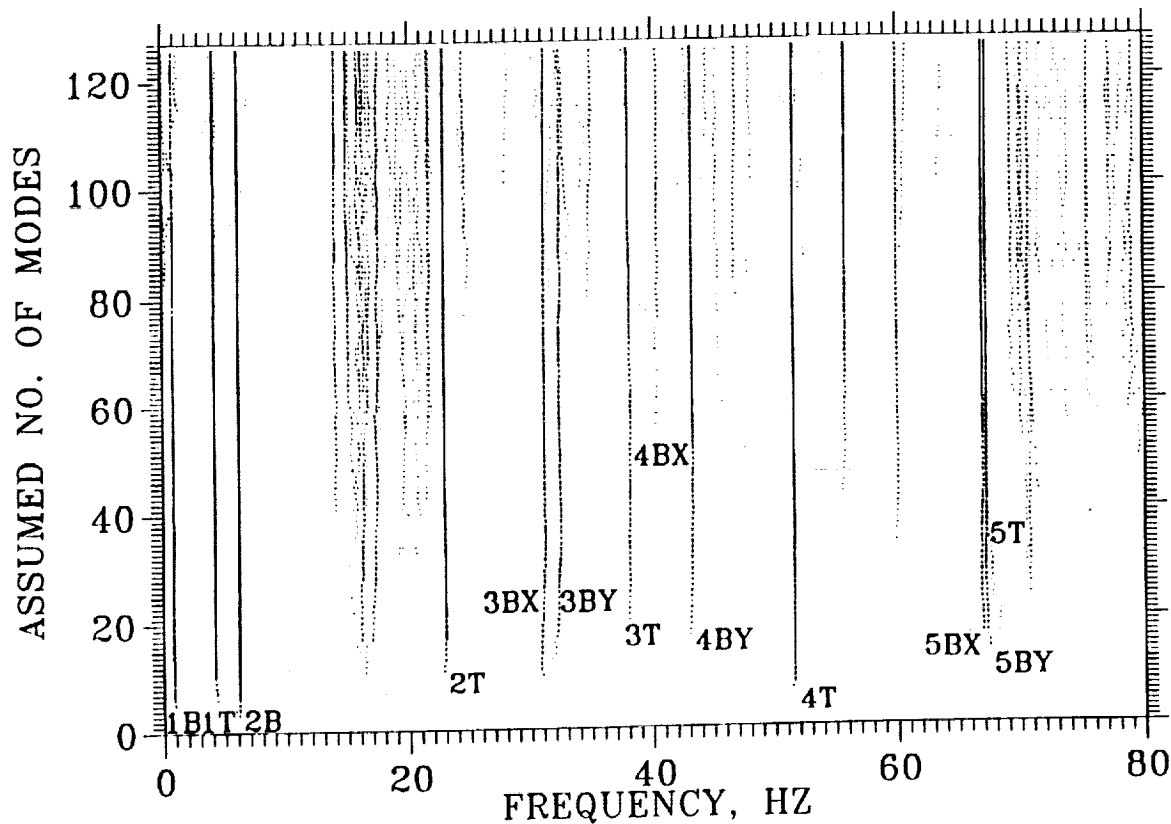With NASTRAN Mode Shapes (Initial Analysis)

Figure 7. Identified Frequencies for Overview Analysis

16
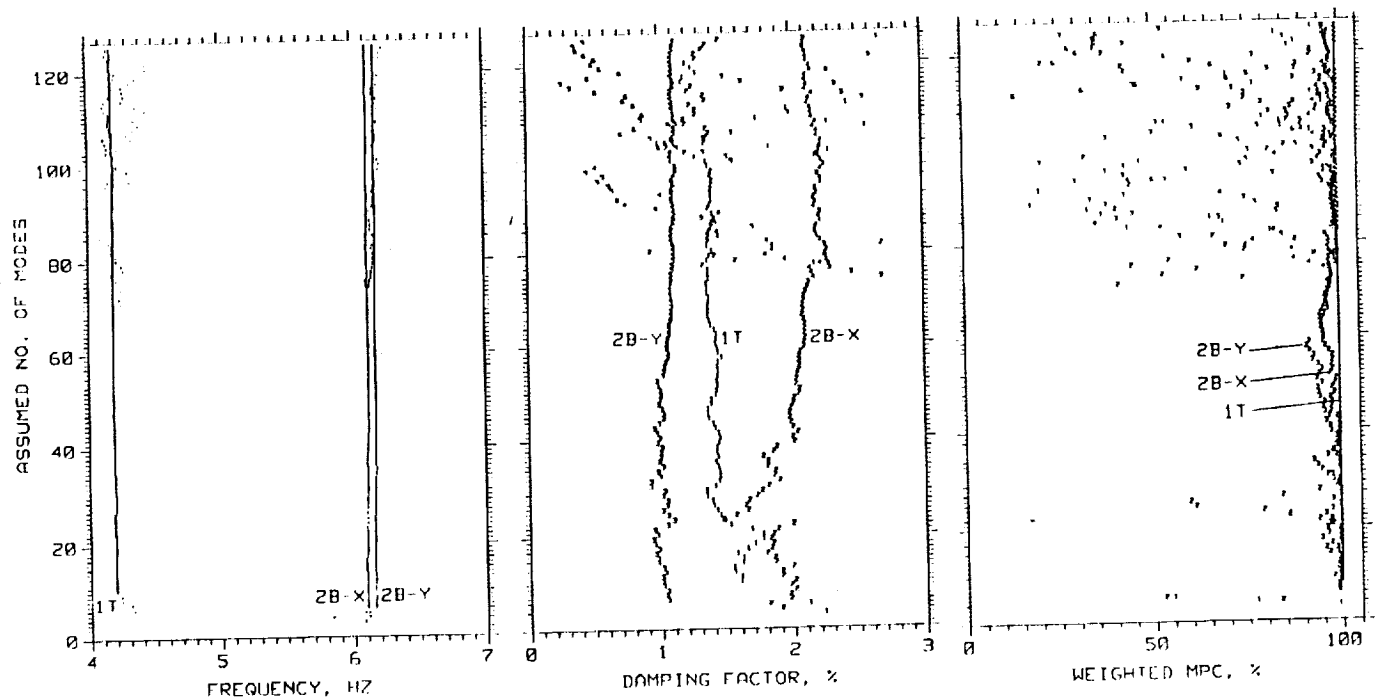
Figure 8. Expanded Plot Near Modes 1T and 2B (Overview Analysis)
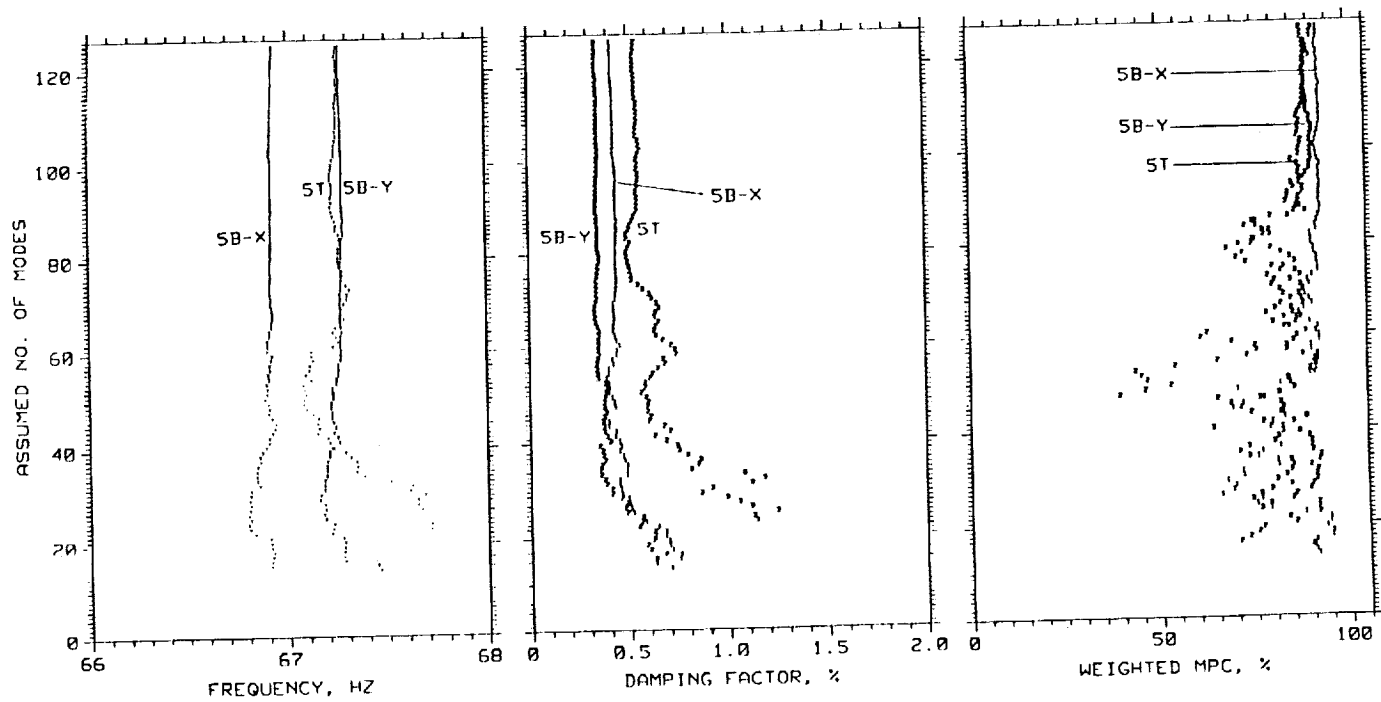
Figure 9. Expanded Plot Near Modes 5B and 5T (Overview Analysis)
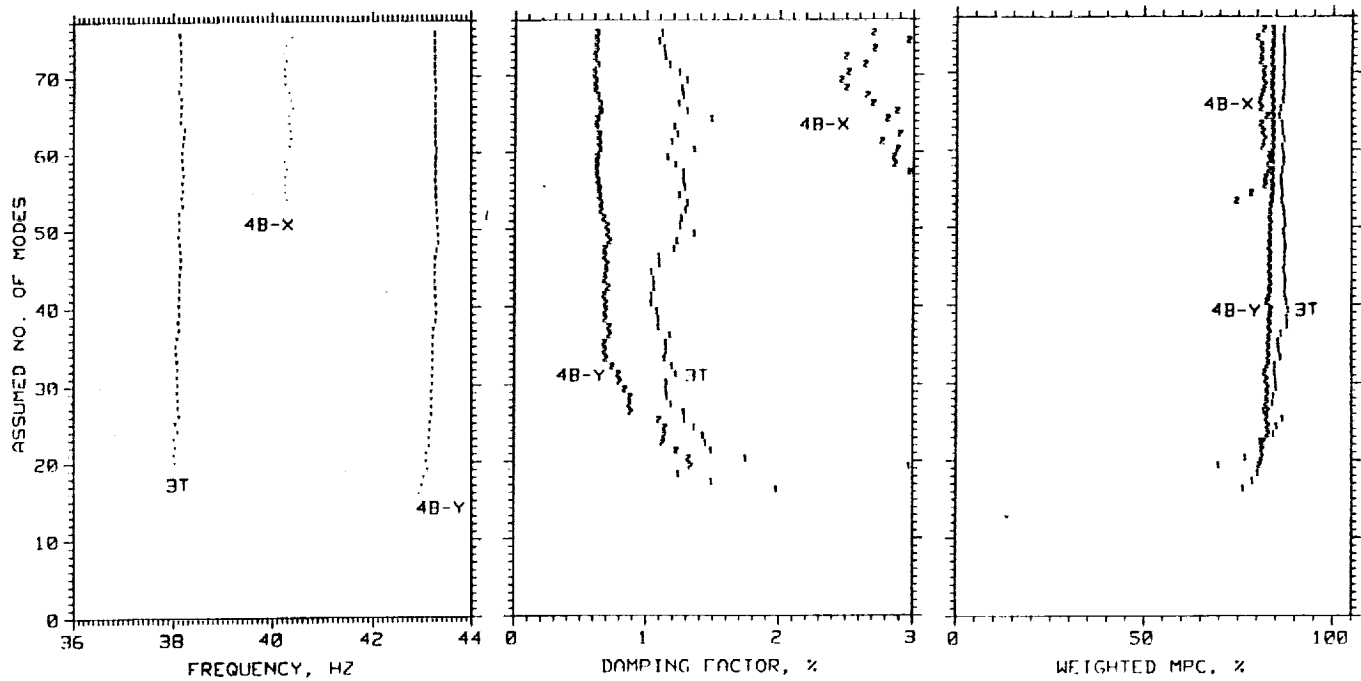
(a) Overview Analysis
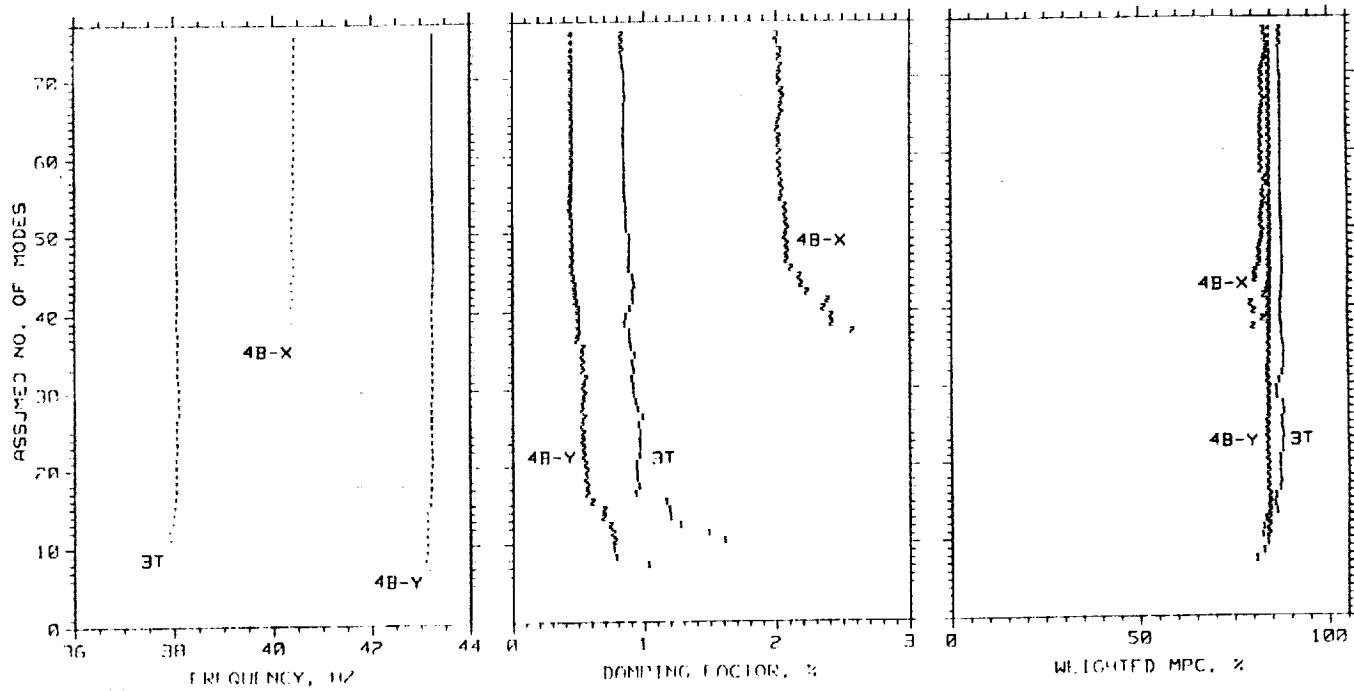
(b) Using Emphasized Data

Figure 10. Improvement of Identification Results
Using Emphasized Data
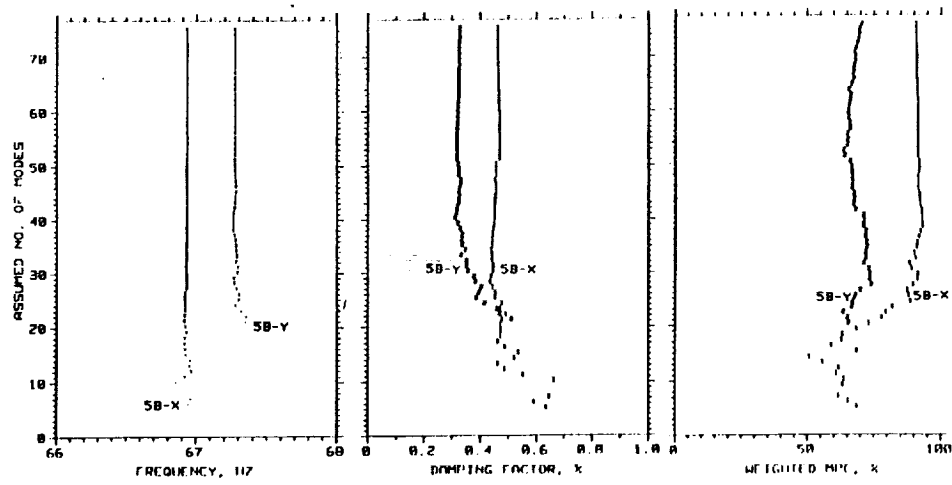
(a) Using Data for Shaker 3 Only
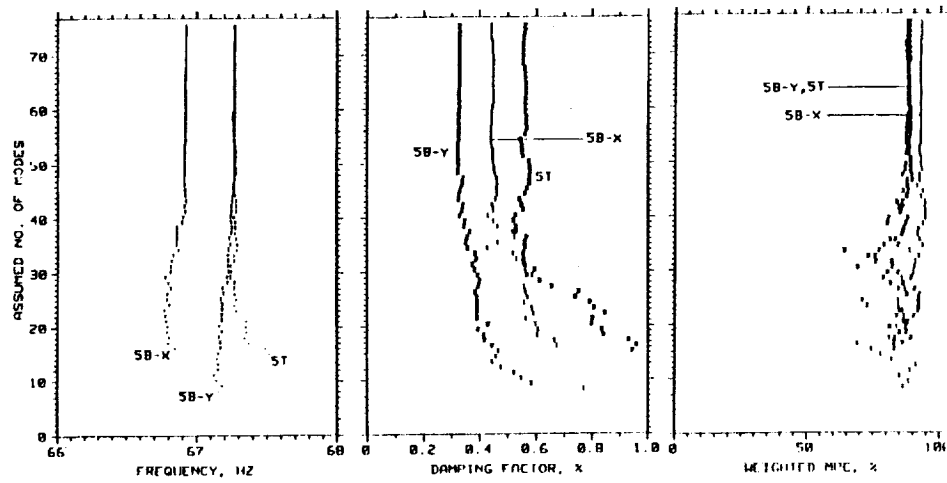
(b) Using Data for All Three Shakers

Figure 11. Multiple-Input Versus Single-Input Analysis
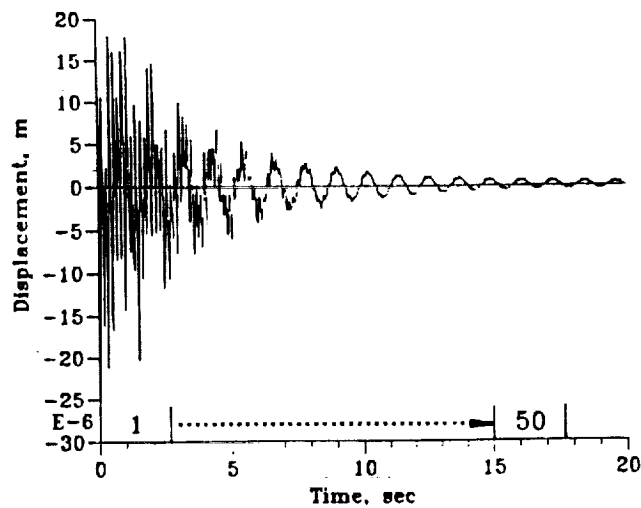
Figure 12. Sliding Time-Window Analysis

19
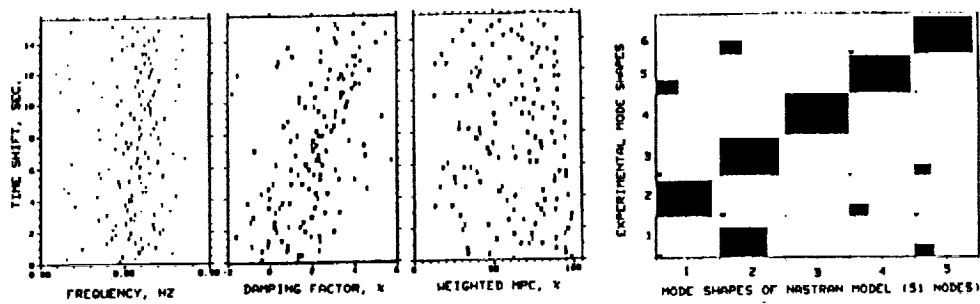
Figure 13. Identification Results Using Sliding Window
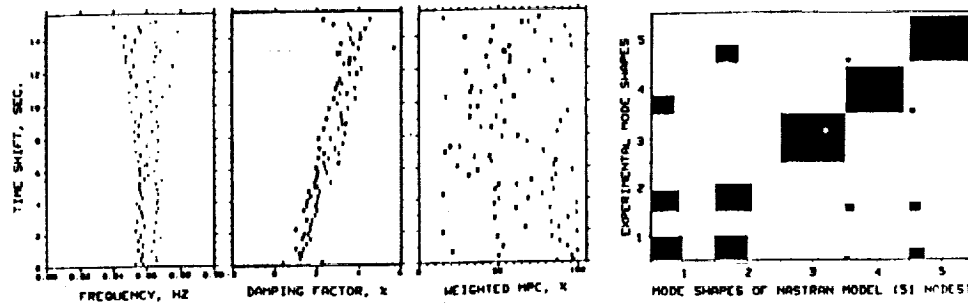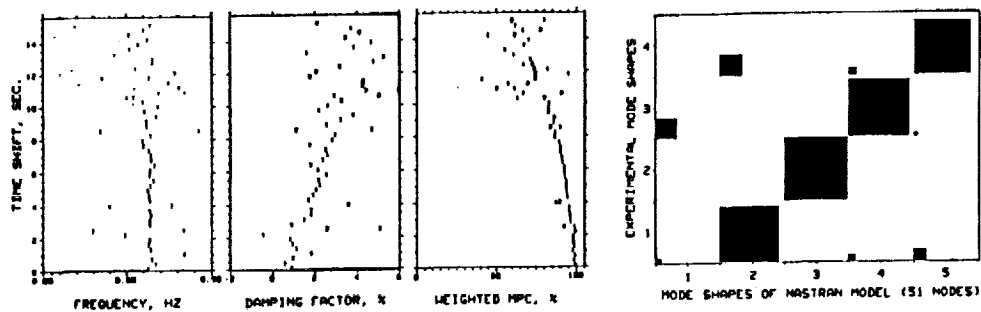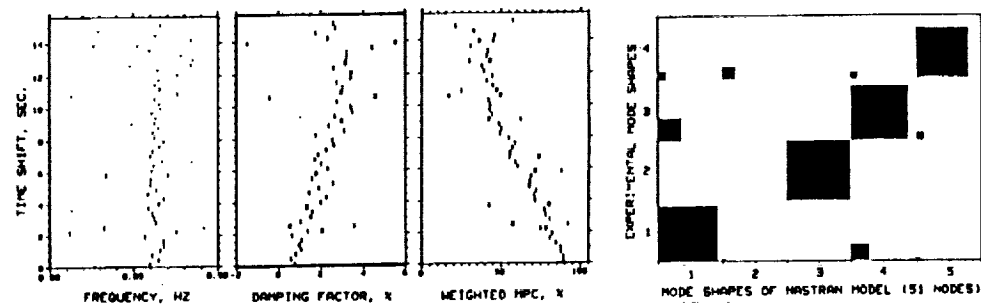Using Data for All Three Shakers

Figure 14. Identification Results Using Sliding Window
Using Data for Shakers 1 and 2

(a) Using Data for Shaker 2 Only

(b) Using Data for Shaker 3 Only

Figure 15. Identification Results Using Sliding Window

20

NASA
National Aeronautics and
Space Administration

Report Documentation Page

1. Report No.	2. Government Accession No.	3. Recipient's Catalog No.
NASA TM-102720		

4. Title and Subtitle	5. Report Date
Modal Identification of a Deployable Space Truss	September 1990
	6. Performing Organization Code

7. Author(s)	8. Performing Organization Report No.
Axel Schenk and Richard S. Pappa	
	10. Work Unit No.
	590-14-61-01

9. Performing Organization Name and Address	11. Contract or Grant No.
NASA Langley Research Center Hampton, VA 23665-5225	
	13. Type of Report and Period Covered

12. Sponsoring Agency Name and Address	Technical Memorandum
National Aeronautics and Space Administration Washington, DC 20546-0001	14. Sponsoring Agency Code

16. Abstract

This paper summarizes work performed under a collaborative research effort between the National Aeronautics and Space Administration (NASA) and the German Aerospace Research Establishment (DLR, Deutsche Forschungsanstalt fur Luft-und Raumfahrt). The objective is to develop and demonstrate advanced technology for system identification of future large space structures. Recent experiences using the Eigensystem Realization Algorithm (ERA) for modal identification of Mini-Mast are reported. Mini-Mast is a 20-meter-long deployable space truss used for structural dynamics and active-vibration-control research at the NASA Langely Research Center. Due to nonlinearities and numerous local modes, modal identification of Mini-Mast proved to be surprisingly difficult. Methods available with ERA for obtaining detailed, high-confidence results are illustrated.

17. Key Words (Suggested by Author(s))		18. Distribution Statement
Large Space Structures Dynamic Testing Modal Identification System Identification Eigensystem Realization Algorithm	Controls-Structures Interaction	Unclassified--Unlimited Subject Category 39

19. Security Classif. (of this report)	20. Security Classif. (of this page)	21. No. of pages	22. Price
Unclassified	Unclassified	21	A03

NASA FORM 1626 OCT 86